A Novel MRI Mapping Technique for Evaluating Bone Bruising Patterns Associated With Noncontact ACL Ruptures

Jay Moran,* BS, Lee D. Katz,†‡ MD, MBA, Christopher A. Schneble,† MD, Don T. Li,* MD, PhD, Joseph B. Kahan,† MD, MPH, Annie Wang,‡ MD, Jack Porrino,‡ MD, Andin Fosam,* BS, Ryan Cheng,§ BA, Peter Jokl,† MD, Timothy E. Hewett,‖ PhD, and Michael J. Medvecky,†¶ MD

Investigation performed at the Department of Orthopaedics and Rehabilitation, Yale School of Medicine, New Haven, Connecticut, USA

Background: Bone bruise patterns in the knee can aid in understanding the mechanism of injury in anterior cruciate ligament (ACL) ruptures. There is no universally accepted magnetic resonance imaging (MRI) mapping technique to describe the specific locations of bone bruises.

Hypothesis: The authors hypothesized that (1) our novel mapping technique would show high interrater and intrarater reliability for the location of bone bruises in noncontact ACL-injured knees and (2) the bone bruise patterns reported from this technique would support the most common mechanisms of noncontact ACL injury, including valgus stress, anterior tibial translation, and internal tibial rotation.

Study Design: Cross-sectional study; Level of evidence, 3.

Methods: Included were 43 patients who underwent ACL reconstruction between 2018 and 2020, with MRI within 30 days of the injury on a 3.0-T scanner, documentation of a noncontact mechanism of injury, and no concomitant or previous knee injuries. Images were retrospectively reviewed by 2 radiologists blinded to all clinical data. The locations of bone bruises were mapped on fat-suppressed T2-weighted coronal and sagittal images using a novel technique that combined the International Cartilage Repair Society (ICRS) tibiofemoral articular cartilage surgical lesions diagram and the Whole-Organ Magnetic Resonance Imaging Scoring (WORMS) mapping system. Reliability between the reviewers was assessed using the intraclass correlation coefficient (ICC), where ICC >0.90 indicated excellent agreement.

Results: The interrater and intrarater ICCs were 0.918 and 0.974, respectively, for femoral edema mapping and 0.979 and 0.978, respectively, for tibial edema mapping. Significantly more bone bruises were seen within the lateral femoral condyle compared with the medial femoral condyle (67% vs 33%; $P < .0001$), and more bruises were seen within the lateral tibial plateau compared with the medial tibial plateau (65% vs 35%; $P < .0001$). Femoral bruises were almost exclusively located in the anterior/central regions (98%) of the condyles as opposed to the posterior region (2%; $P < .0001$). Tibial bruises were localized to the posterior region (78%) of both plateaus as opposed to the anterior/central regions (22%; $P < .0001$).

Conclusion: The combined mapping technique offered a standardized and reliable method for reporting bone bruises in noncontact ACL injuries. The contusion patterns identified using this technique were indicative of the most commonly reported mechanisms for noncontact ACL injuries.

Keywords: anterior cruciate ligament; noncontact mechanism; bone bruise; MRI; bone marrow edema

Anterior cruciate ligament (ACL) injuries can occur via either a contact or a noncontact mechanism. Noncontact mechanisms are the most common and occur when a person is changing direction during sudden landing, pivoting, or deceleration.[17,18,23] Contact ACL injuries typically involve a direct blow to the knee or the body and can occur in various manners.[23] However, noncontact injuries are believed to be more preventable and thus are the focus of various injury prevention programs that are predicated on a thorough understanding of their mechanism.[4,11,21]

In ACL ruptures, occult osseous injuries are frequently identified on magnetic resonance imaging (MRI) scans and are considered areas of poorly marginated signal intensity altercations in both the cancellous bone and marrow.[16] Such appearances are thought to represent areas of hemorrhage, edema, or hyperemia secondary to trabecular

The Orthopaedic Journal of Sports Medicine, 10(4), 23259671221088936
DOI: 10.1177/23259671221088936

injury.[16] These injuries are termed *edema-like marrow signal intensity*[9] or *bone marrow edema (bone bruises)* within the tibia and femur and occur in 80% to 99% of acute ACL injuries.[10,13,24] During ACL injury, large external forces on the knee result in high-energy compressive and shear forces between the femoral and tibial articular cartilage.[13,24] The compression results in impaction, producing tibiofemoral compartment bone bruising that is evident on MRI scans. The femoral and tibial bone bruising seen after ACL injury can represent a compressive "footprint" from the time of injury and provides a greater insight into the mechanism of injury.[5,13,17,20,24]

Currently, there are limited accepted mapping methods to describe the locations of bone bruises within the acutely injured knee. Multiple studies have described bone bruise patterns in a general fashion, localized to either the lateral or medial portions of the femur and tibia with little specificity as to the location with the respective condyles in both the coronal and sagittal planes.[13,24] Previous systematic reviews have advocated future studies to develop reliable, standardized mapping techniques that partition the femur and tibia to yield more precise, reproducible locations of bone bruises.[13,24] A standardized mapping technique with sufficient reliability would provide a consistent method to describe these bone bruise patterns and alleviate further variability in how these contusions are reported. Such a method could provide more useful and consistently descriptive bone bruise information regarding correlations with concomitant injuries and inferred mechanisms of injury that led to the resultant marrow edema.

The purpose of this study was to develop a novel mapping technique from a combination of the tibiofemoral articular cartilage surgical lesions diagram from the International Cartilage Repair Society (ICRS) as well as the Whole-Organ Magnetic Resonance Imaging Scoring (WORMS) mapping system, which included femoral and tibial partitions to describe the locations and degree of osteoarthritis within the knee.[1,14] We hypothesized that our mapping technique would show high interrater and intrarater reliability, defined by an intraclass correlation coefficient (ICC) >0.90, indicating excellent agreement for the location of bone bruises in noncontact ACL-injured knees. A secondary hypothesis was that the bone bruise patterns reported from this technique would support the most common mechanisms of noncontact ACL injury in the literature, including valgus stress, anterior tibial translation, and internal tibial rotation.

METHODS

The study protocol received institutional review board approval. A total of 116 patients were identified as having undergone isolated ACL reconstructive surgery between 2018 and 2020 by a single orthopaedic surgeon (M.J.M.). Of these, 43 patients met the following inclusion criteria for this study: (1) <30 days between date of the reported injury and date of the MRI, (2) T2-weighted fat-suppressed MRI sequences available in both the coronal and sagittal planes, (3) documented mechanism of injury, (4) noncontact injury, and (5) no documentation of previous ACL injury or concomitant posterolateral injury. The mechanism of injury was recorded as either noncontact or contact based on the patient's account of the injury. Patient age at time of MRI, sex, date of injury, and date of MRI were also recorded. Patient consent was not granted due to IRB approval and the use of anonymized data.

All 43 patients underwent MRI on a 3.0-T scanner according to the standard knee protocol at our institution. All of the imaging studies were independently, retrospectively reviewed by 2 board-certified musculoskeletal radiologists, one with 7 years of clinical experience (A.W.) and the other with 39 years of clinical experience (L.D.K.). Only fat-suppressed T2-weighted coronal and sagittal images were reviewed to determine the location of bone marrow edema. The sequence specifics for the images were an average repetition time of 6500 ms, echo time of 45 ms, field of view of 14 to 16 cm, and resolution of 256 × 256.

Development of the Mapping Technique

The novel mapping technique developed in the present study represents a combination of the ICRS tibiofemoral articular cartilage surgical lesions diagram and the WORMS mapping system (Figure 1). In contrast to previous mapping studies,[3,6-8,13,15,17,19,24] we used a mapping technique with a more well-defined, greater number of zones to describe the location of contusions, as illustrated in Figures 2 to 4.

Coronal Plane Mapping Regions

In the coronal plane, the femur and tibia were separated into medial and lateral halves by a straight sagittal line (green line in Figure 2) through the midaspect of the intercondylar notch. The peripheral medial and lateral zones were defined as the region between the periphery and the

¶Address correspondence to Michael J. Medvecky, MD, Department of Orthopaedics and Rehabilitation, Yale School of Medicine, New Haven, CT 06511, USA (email: michael.medvecky@yale.edu) (Twitter: @JayMoran25, @OrthoAtYale, @Hewett1Tim, @MichaelMedveck1).
*Yale School of Medicine, New Haven, Connecticut, USA.
†Department of Orthopaedics and Rehabilitation, Yale School of Medicine, New Haven, Connecticut, USA.
‡Department of Radiology and Biomedical Imaging, Yale School of Medicine, New Haven, Connecticut, USA.
§Yale University, New Haven, Connecticut, USA.
‖Hewett Global Consulting, Rochester, Minnesota, USA.
Final revision submitted December 17, 2021; accepted January 21, 2022.
The authors declared that they have no conflicts of interest in the authorship and publication of this contribution. AOSSM checks author disclosures against the Open Payments Database (OPD). AOSSM has not conducted an independent investigation on the OPD and disclaims any liability or responsibility relating thereto.
Ethical approval for this study was obtained from Yale University (protocol No. 2000028578).

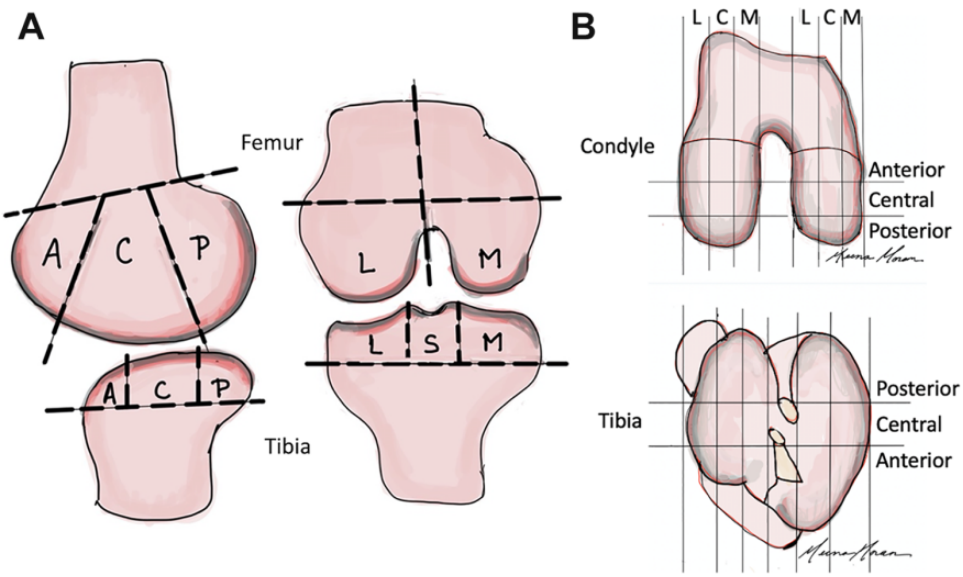

Figure 1. (A) Illustration of the Whole-Organ Magnetic Resonance Imaging Scoring mapping system in both the sagittal and coronal directions for the femur and tibia. (B) Illustration of the International Cartilage Repair Society method for mapping cartilaginous lesions on the condyle and tibia. A, anterior; C, central; L, lateral; M, medial; P, posterior; S, spine.

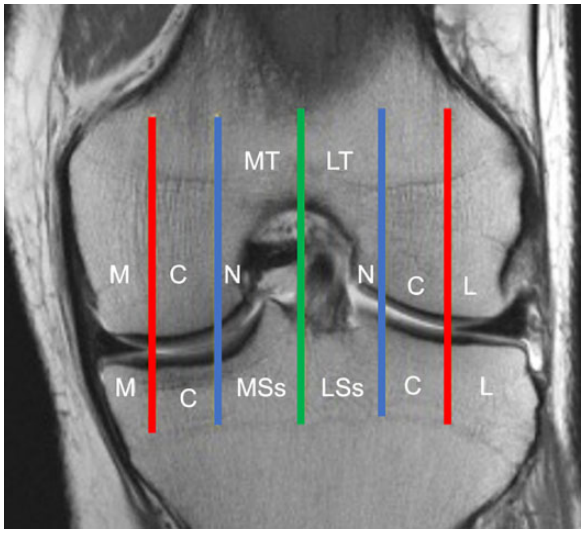

Figure 2. T2-weighted coronal magnetic resonance imaging scan with distinct femoral and tibial zones used to record the location of the lesions in the coronal plane. The red lines represent the inner/free margins of the meniscus, the blue lines represent the upslope of the medial and lateral tibial spines, and the green line represents the central sagittal line dividing the femur and tibia into medial and lateral compartments. C, central; L, lateral; LSs, lateral subspine; LT, lateral trochlea; M, medial; MT, medial trochlea; MSs, medial subspine; N, notch.

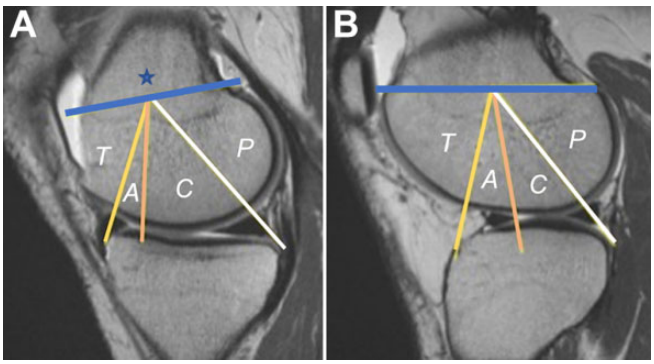

Figure 3. Sagittal proton-density magnetic resonance imaging scans of the (A) medial knee and (B) lateral knee divided into 4 zones for localization. The sagittal landmarks for the femoral zones were first defined by a line drawn horizontally in the anteroposterior plane connecting the most proximal aspect of the articular cartilage of each femoral condyle (blue line). The central axis of the femur in the sagittal plane was considered to be at the middle of this line (blue star in image A). Lines extending from the central axis to the most anterior (yellow line) and posterior (white line) aspects of the tibial plateau defined the trochlear (T), central (C), and posterior femoral (P) zones. The central femoral zone was further subdivided into an anterior central zone (A), which was defined as the area between the line separating the trochlear and central zones (yellow line) and a second line extending from the central axis to the most anterior aspect of the weightbearing region of the articular cartilage contact of the femur and tibia (orange line).

inner/free margin of the medial and lateral menisci (as defined by the red lines in Figure 2), respectively. The resultant zones were referred to as the femoral-medial-medial (FMM), femoral-lateral-lateral (FLL), tibia-medial-medial (TMM), and tibia-lateral-lateral (TLL) zones.

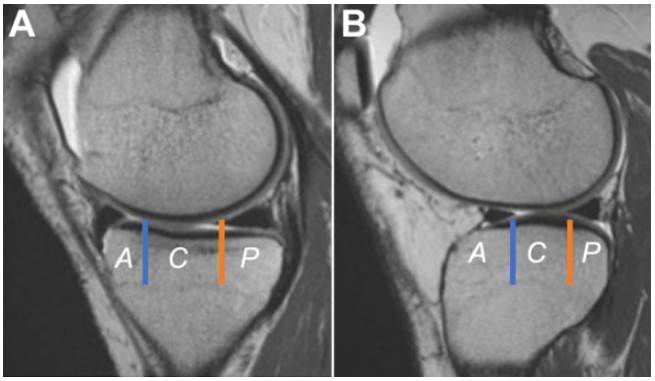

Figure 4. Sagittal proton-density magnetic resonance imaging scans of the (A) medial knee and (B) lateral knee divided into 3 zones for localization. The central zone (C) was defined by the most anterior aspect of the inner rim/free edge of the posterior horn of each meniscus (orange line) and the most anterior aspect of the contact surface of the tibiofemoral articulation (blue line). The anterior (A) and posterior (P) zones were those areas at the anterior and posterior peripheries of the central zone, respectively.

The more central weightbearing zones included the medial femoral condyle (MFC) central (referred to as femoral-medial-central), lateral femoral condyle (LFC) central (referred to as femoral-lateral-central [FLC]), medial tibia plateau central (referred to as tibia-medial-central [TMC]), and lateral tibia plateau central (referred to as tibia-lateral-central [TLC]) and were defined by the area between the inner/free margins of the menisci (red lines in Figure 2) and the upslope of the medial and lateral tibial spines (blue lines in Figure 2).

The region between the upslope of the medial and lateral tibial spines (as defined by the blue lines in Figure 2) and the central sagittal line dividing the femur and tibia into medial and lateral compartments (green line in Figure 2) defined the femoral notch zones (referred to as femoral-medial-notch and femoral-lateral-notch) and the subspine zones on the tibia (referred to as tibia-medial-subspine [TMS] and tibia-lateral-subspine [TLS]).

The femoral notch zones were further subdivided into medial and lateral trochlear regions with the same borders in the coronal plane as the femoral notch zones but demarcated by the proximal aspect of the trochlear notch. These 2 zones were referred to as the femoral-medial-trochlea and femoral-lateral-trochlea zones.

Sagittal Plane Mapping Regions

After the coronal locations of lesions were recorded, the sagittal plane MRI scan was used to define the anteroposterior location of the bone marrow edema within the femur and tibia.

Femoral Zones. The sagittal landmarks for the femoral zones were defined as the trochlear anterior central, central, and posterior femoral regions, as shown in Figure 3.

TABLE 1
Distribution of Total Bone Lesions in the Medial and Lateral Compartment Zones for the Femur and Tibia[a]

Site	Medial Zone	Lateral Zone	*P*
Femur	33 (33)	66 (67)	**<.0001**
Tibia	63 (35)	118 (65)	**<.0001**

[a]Data are reported as No. (%) of lesions. Bolding indicates statistically significant difference between the medial and lateral zones ($P < .05$).

Tibial Zones. The tibial zones on the sagittal image were divided into anterior, central, and posterior regions, as shown in Figure 4.

Data Collection

The intersecting coronal-sagittal location of each lesion was recorded. If the lesion was located across multiple zones, each individual zone to which it extended was counted. Similarly, if multiple lesions were present, edema was counted to the individual zone(s) it spanned. The signal intensity and volume of the lesions were not recorded.

The same data set was read twice by each radiologist, and the length of time between each reading was 6 weeks. The primary outcome, intrarater and interrater reliability for mapping the location of the bone bruises, was assessed using intraclass correlation coefficients (ICCs). ICC values were interpreted as follows: <0.5 poor, 0.5 to 0.75 moderate, 0.75 to 0.9 good, and >0.90 excellent. The secondary outcome, the analysis of bone bruise patterns, was assessed using chi-square tests to analyze significant bone bruise frequencies in a contingency table to describe the mechanisms of injury. A Z test was used to compare 2 population proportions for categorical variables. All statistics were performed using Excel (Microsoft Corp). The threshold for significance was set at $P < .05$.

RESULTS

The interrater and intrarater ICCs for assessment of the femoral map MRI readings were 0.918 and 0.974, respectively. Similarly, the interrater and intrarater ICCs for assessment of the tibial map MRI readings were 0.979 and 0.978, respectively. All ICC values indicated excellent reliability for reporting the locations of bone marrow edema in ACL injuries.

The mean ± standard deviation age of our cohort was 27.5 ± 14.9 years, and 42% of participants were female. The mean time between the injury and MRI was 11.8 ± 8.2 days. A total of 40 knees (93%) had at least 1 bone contusion on MRI scans.

In total, 81% of knees (n = 35) had at least 1 bone lesion at the LFC, whereas 63% of knees (n = 27) had at least 1 lesion at the MFC; these differences were not statistically significant ($P = .0963$). Similarly, no statistically significant difference was found in the number of knees with at

least 1 lesion on the lateral (LTP) versus medial tibial plateau (MTP) (82% vs 64%; $P = .0969$).

When assessing total lesions within the cohort, we found significantly more lesions at the LFC compared with the MFC (67% vs 33%; $P < .0001$). Likewise, significantly more lesions were found on the LTP compared with the MTP (65% vs 35%; $P < .0001$) (Table 1).

With regard to the sagittal plane orientation of lesions, 98% of femoral condyle lesions (both lateral and medial) occurred in the anterior and central regions, whereas 2% occurred in the posterior region of the femoral condyles ($P < .0001$). The distribution of tibial lesions had an inverse pattern compared with that of femoral lesions, with lesions affecting the posterior zone (78%) more than the anterior/central zones (22%; $P < .0001$) (Table 2).

When we localized intersecting femoral lesions in both the coronal and sagittal planes, we found that within the LFC, the majority of lesions occurred at the anterior-FLL (60%) and anterior-FLC (40%) zones. On the MFC, the majority of lesions were localized to the central-FMM (47%) zone (Figure 5).

The bruising patterns on the tibia were diffusely distributed from medial to lateral ($P = .6086$); however, the lesions were significantly localized to the posterior region of the tibia ($P < .0001$). On the posteromedial side, 35%, 40%, and 37% of knees had lesions localized to the posterior-TMM, posterior-TMC, and posterior-TMS zones, respectively. Similarly, on the posterolateral side, 67%, 77%, and 72% of knees had lesions localized to the posterior-TLS, posterior-TLC, and posterior-TLL zones, respectively (Figure 6).

TABLE 2
Distribution of the Total Bone Lesions at the Femur and Tibia in the Anterior/Central and Posterior Zones[a]

Site	Anterior/Central Zone	Posterior Zone	*P*
Femur	88 (98)	2 (2)	**<.0001**
Tibia	40 (22)	141 (78)	**<.0001**

[a]Data are reported as No. (%) of lesions. Bolding indicates statistically significant difference between the anterior/central and posterior zones ($P < .05$).

DISCUSSION

The most important finding of this study was that our novel mapping technique showed excellent reliability for determining the location of bone bruises in noncontact ACL injuries, which confirmed our primary hypothesis. Our secondary hypothesis was also supported, as the most common mechanisms of noncontact ACL injury inferred from the location of these bone bruises were valgus stress, anterior tibial translation, and internal tibial rotation. Currently, universally accepted mapping techniques for reporting the location of bone bruises in the acutely injured knee are limited. The results of this study show that our standardized MRI mapping technique can be used in future bone bruise studies, with greater reliability than previously reported in the literature.

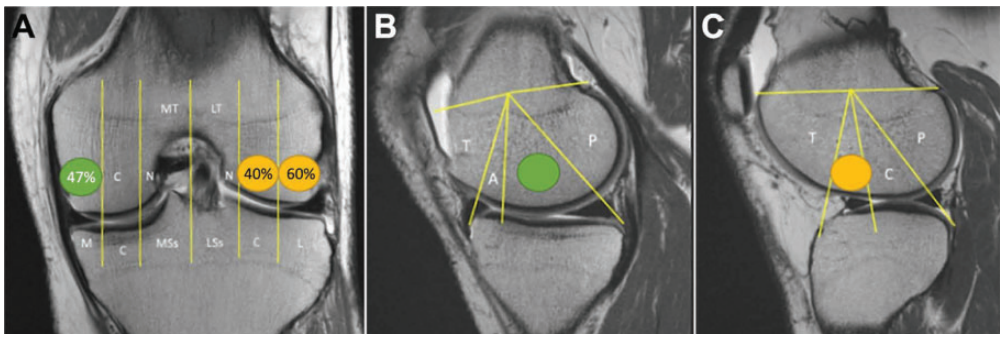

D	Femur							
	FMM	FMC	FMN	FMT	FLT	FLN	FLC	FLL
Trochlear	7%	2%	2%	2%	0%	0%	0%	7%
Anterior	2%	2%	0%	0%	5%	9%	40%	60%
Central	47%	2%	2%	2%	2%	2%	9%	19%
Posterior	2%	2%	0%	0%	0%	0%	0%	0%

Figure 5. (A) Coronal, (B) medial sagittal, and (C) lateral sagittal proton-density magnetic resonance imaging scans denoting the femoral zones with the greatest number of lesions. The colored circles represent the zones where the greatest number of contusions were identified within the respective medial (green) and lateral (yellow) femoral condyle coronal zones and their location in the sagittal plane. (D) Map detailing the percentage of knees with bone lesions at a given femoral zone, with the values in the green and yellow cells denoting the highest frequencies as shown in (A). *P* value for the whole table = .00023 (χ^2 test). A, anterior; C, central; F, femoral; L, lateral; LSs, lateral subspine; LT, lateral trochlea; M, medial; MSs, medial subspine; MT, medial trochlea; N, notch; P, posterior; T, trochlear.

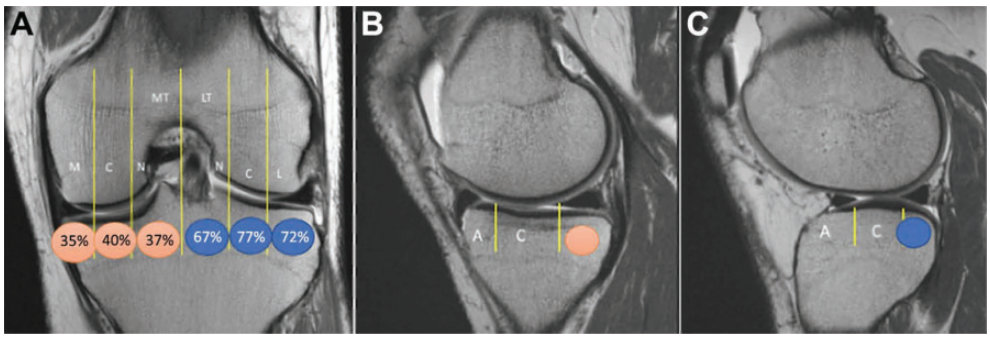

D	Tibia					
	TMM	TMC	TMSs	TLSs	TLC	TLL
Anterior	7%	5%	5%	2%	2%	2%
Central	7%	7%	5%	12%	21%	19%
Posterior	35%	40%	37%	67%	77%	72%

Figure 6. (A) Coronal, (B) medial sagittal, and (C) lateral sagittal proton-density magnetic resonance imaging scans denoting the tibial zones with the greatest number of lesions. The colored circles represent the zones where the greatest number of lesions were identified within the respective medial (pink) and lateral (blue) tibial plateau coronal zones and their location in the sagittal plane. (D) Map detailing the percentage of knees with bone lesions at a given tibial zone, with the values in the pink and blue cells denoting the highest frequencies as shown in (A). *P* value for the whole table = .6086 (χ^2 test). A, anterior; C, central; L, lateral; LT, lateral trochlea; M, medial; MT, medial trochlea; N, notch; T, tibial.

Patel et al[13] conducted one of the largest systematic reviews for bone bruising in the context of ACL injury and noted that few studies consistently or precisely reported the location of contusions. Most studies localize edema to the LFC, LTP, MFC, and/or MTP but do not further describe the location within these broad categories.[13,17,20,22,24] The proposed mapping technique in our study was built using components of the ICRS and WORMS tibiofemoral mapping systems.[1,14] Both these systems have been used to assess the presence and severity of cartilaginous lesions, meniscal tears, and bone marrow lesions in knees with osteoarthritis with excellent reliability. In the coronal plane, the WORMS mapping method divides the femur into only 2 compartments, medial and lateral, and the tibia into 2 primary compartments, medial and lateral, with a smaller accessary region known as the tibial spine. In the sagittal plane, the aforementioned method divides the femur and the tibia into more compartments, with 3 regions in each described. Compared with the WORMS, the ICRS method has more zones in the coronal and sagittal planes but with a mapping reference less amenable to positioning and sequencing as seen in typical knee MRI scan with the knee in full extension.[1,14] The mapping technique used and proposed in the current study combines the zones from the WORMS and the ICRS methods. We further divided the distal femur into 8 coronal and 4 sagittal zones and the proximal tibia into 6 coronal and 3 sagittal zones. The expansion of the coronal divisions was thought to provide a more precise 2-dimensional description of marrow edema when combined with the respective location from anterior to posterior in the sagittal plane. This increased degree of precise localization of marrow edema in the acutely injured knee may help further elucidate mechanisms of injury. Additionally, future studies can focus on how the specific locations of bone bruises relate to concomitant injuries of the menisci or alternative ligamentous and tendinous structures about the knee, which may correlate to the respective zones.

Viskonstas et al[20] reported on bone contusions in ACL injuries using a version of the ICRS mapping scheme, with 2 coronal zones and 3 sagittal zones, and reported good reliability (ICC = 0.67) for the location of the contusions. In the present study, using our newly developed mapping strategy, 2 board-certified musculoskeletal radiologists conducted the readings, with ICCs for both intrarater and interrater reliability >0.90, indicating excellent and superior reliability for this method to describe locations of ACL bone marrow edema in noncontact injuries. In addition to excellent reliability, the mapping system proposed in the current study relies on basic MRI techniques that are readily available and do not require computer-based calculations or computing software. Although other highly technical mapping techniques for ACL edema patterns, such as the one described by Shi et al,[17] have achieved excellent reliability, they often require the use of extensive computer software and entail a steeper learning curve.

The bone bruising patterns identified in the current study are consistent with the inferred mechanisms of noncontact ACL injury reported within the literature, further supporting the use of our proposed mapping technique. We found significantly more lesions within the lateral tibiofemoral compartment of the knee compared with the medial tibiofemoral compartment, indicating that high-energy collisions between the LFC and LTP occur more frequently

than do those of the MFC and MTP at the time of injury.[13,17,20,22,24] The increased frequency of lateral compartment bruising compared with medial compartment bruising in noncontact ACL injuries in our study is consistent with findings of previous ACL bone contusion studies.[2,5,7,10,12,13,17,24] This edema pattern has been attributed to a valgus moment of the knee during injury, causing lateral-sided compression of the femur and tibia, resulting in more high-impact collisions within the lateral tibiofemoral compartment compared with the medial tibiofemoral compartment.[2,5,7,10,12,13,17,24]

Using sagittal plane analysis, we found that the bone bruise patterns on both femoral condyles were localized to the anterior and central regions whereas the bruising patterns on both tibia plateaus were localized to the posterior region. These findings indicate that at some point during the injury, the posterior regions of both tibia plateaus collided with the anterior/central regions of the femoral condyles on both the medial and lateral sides. In order for these compartments to come into high-energy contact, the posterior tibia must translate anteriorly relative to the femur on both the medial and lateral sides.[13,17,20,24] This sagittal bruising pattern is in agreement with that reported in previous studies that have described anterior tibial translation.[17,20]

The difference in sagittal bruising patterns on the MFC and LFC provides insight into the degree of internal or external rotation of the tibia.[13,17,20,24] Lesions were localized to the anterior region on the LFC. In contrast, the contusions observed on the MFC were localized to the central region. With pure anterior translation and no internal or external tibial rotation, the sagittal bruising patterns on the MFC and LFC would be localized to the same sagittal region.[17,20] However, anterior translation with internal rotation of the tibia would cause the posterior region of the LTP to collide with the LFC more anteriorly than the collision between the posterior region of the MTP and the MFC. As the tibia internally rotates, the posterior region of the LTP rotates anteriorly.[20] This results in different collision points and sagittal bruising on the MFC and LFC within the extended knee. Our observation of tibial rotation during noncontact ACL injury is in accord with recent studies reporting similar findings.[13,17,20,24]

The bone bruising patterns identified in our study suggest that valgus stress and anterior translation with internal tibial rotation occur in many noncontact ACL injuries. These observations have been reported in previous reports, further supporting the use of our mapping technique.[15,17,19,20]

Limitations

There are certain limitations of our study. Our cohort was relatively small, with 43 patients; however, this study represents a single-surgeon series with statistically significant data reported. Additionally, bone marrow edema can be difficult to accurately characterize on MRI scan and can be misinterpreted when the time between injury and MRI is delayed. We sought to obviate this limitation by including only those patients with MRI performed within 30 days from the date of injury. The average time between the initial injury and MRI in our study was 11 days, and we demonstrated excellent interobserver reliability. However, when considering the agreement between the readers, it is important to note that all MRI was conducted on a 3.0-T scanner. Given that a 1.5-T scanner is used in most clinical settings, this could affect the generalizability of our reported reliability and findings, as 3.0-T scanners provide greater resolution and higher quality images. Whether the bone bruises occurred at the time of ACL injury or whether they were a consequence of the sequelae afterward may represent a limitation of using bone bruises to infer mechanisms of injury. However, it is certain that a high-energy tibiofemoral impact at the time bone bruising occurred, and a greater frequency in particular bruise distributions would indicate a common joint alignment at the time of impact.

We did not evaluate contact ACL injuries in our study, and therefore, we have not presented a comprehensive overview of contusion patterns that occur in all forms of ACL injury. However, we deliberately elected to focus on noncontact ACL injury, as this in general is considered preventable, and a thorough understanding of mechanism is essential in altering preventive strategies. In addition, we did not assess the influence of bone marrow edema patterns with additional injuries of the menisci or alternative ligaments and tendons about the knee. Future research using our proposed mapping strategy could be aimed at contrasting our results with results for patients who sustain contact ACL injuries to determine how these 2 patterns may differ, as well as evaluating the influence of precise contusion patterns with concomitant injuries around the knee.

CONCLUSION

The combined mapping technique offered a standardized and reliable method for reporting bone marrow edema patterns in noncontact ACL injuries. The bone bruise patterns identified using this technique supported the most commonly reported mechanisms for noncontact ACL injuries, including valgus stress, anterior tibial translation, and internal tibial rotation.

ACKNOWLEDGMENT

The authors thank Meena S. Moran, MD, for her artwork contributions (Figure 1).

REFERENCES

1. Brittberg M, Winalski CS. Evaluation of cartilage injuries and repair. *J Bone Joint Surg Am*. 2003;85-A(suppl 2):58-69.
2. Chin YC, Wijaya R, Chong Ie R, Chang HC, Lee YH. Bone bruise patterns in knee injuries: where are they found? *Eur J Orthop Surg Traumatol*. 2014;24(8):1481-1487.
3. Davies NH, Niall D, King LJ, Lavelle J, Healy JC. Magnetic resonance imaging of bone bruising in the acutely injured knee—short-term outcome. *Clin Radiol*. 2004;59(5):439-445.
4. Hewett TE, Myer GD, Ford KR, et al. Biomechanical measures of neuromuscular control and valgus loading of the knee predict anterior

cruciate ligament injury risk in female athletes: a prospective study. *Am J Sports Med*. 2005;33(4):492-501.
5. Kaplan PA, Gehl RH, Dussault RG, Anderson MW, Diduch DR. Bone contusions of the posterior lip of the medial tibial plateau (contrecoup injury) and associated internal derangements of the knee at MR imaging. *Radiology*. 1999;211(3):747-753.
6. Kia C, Cavanaugh Z, Gillis E, et al. Size of initial bone bruise predicts future lateral chondral degeneration in ACL injuries: a radiographic analysis. *Orthop J Sports Med*. 2020;8(5):2325967120916834.
7. Kim SY, Spritzer CE, Utturkar GM, Toth AP, Garrett WE, DeFrate LE. Knee kinematics during noncontact anterior cruciate ligament injury as determined from bone bruise location. *Am J Sports Med*. 2015; 43(10):2515-2521.
8. Mair SD, Schlegel TF, Gill TJ, Hawkins RJ, Steadman JR. Incidence and location of bone bruises after acute posterior cruciate ligament injury. *Am J Sports Med*. 2004;32(7):1681-1687.
9. Maraghelli D, Brandi ML, Matucci Cerinic M, Peired AJ, Colagrande S. Edema-like marrow signal intensity: a narrative review with a pictorial essay. *Skeletal Radiol*. 2021;50(4):645-663.
10. Owusu-Akyaw KA, Kim SY, Spritzer CE, et al. Determination of the position of the knee at the time of an anterior cruciate ligament rupture for male versus female patients by an analysis of bone bruises. *Am J Sports Med*. 2018;46(7):1559-1565.
11. Padua DA, DiStefano LJ, Hewett TE, et al. National Athletic Trainers' Association position statement: prevention of anterior cruciate ligament injury. *J Athl Train*. 2018;53(1):5-19.
12. Papakonstantinou O, Chung CB, Chanchairujira K, Resnick DL. Complications of anterior cruciate ligament reconstruction: MR imaging. *Eur Radiol*. 2003;13(5):1106-1117.
13. Patel SA, Hageman J, Quatman CE, Wordeman SC, Hewett TE. Prevalence and location of bone bruises associated with anterior cruciate ligament injury and implications for mechanism of injury: a systematic review. *Sports Med*. 2014;44(2):281-293.
14. Peterfy CG, Guermazi A, Zaim S, et al. Whole-organ magnetic resonance imaging score (WORMS) of the knee in osteoarthritis. *Osteoarthritis Cartilage*. 2004;12(3):177-190.
15. Quatman CE, Kiapour A, Myer GD, et al. Cartilage pressure distributions provide a footprint to define female anterior cruciate ligament injury mechanisms. *Am J Sports Med*. 2011;39(8):1706-1713.
16. Sanders TG, Medynski MA, Feller JF, Lawhorn KW. Bone contusion patterns of the knee at MR imaging: footprint of the mechanism of injury. *Radiographics*. 2000;20(suppl 1):S135-S151.
17. Shi H, Ding L, Jiang Y, et al. Bone bruise distribution patterns after acute anterior cruciate ligament ruptures: implications for the injury mechanism. *Orthop J Sports Med*. 2020;8(4):2325967120911162.
18. Shin CS, Chaudhari AM, Andriacchi TP. The effect of isolated valgus moments on ACL strain during single-leg landing: a simulation study. *J Biomech*. 2009;42(3):280-285.
19. Song GY, Zhang H, Wang QQ, Zhang J, Li Y, Feng H. Bone contusions after acute noncontact anterior cruciate ligament injury are associated with knee joint laxity, concomitant meniscal lesions, and anterolateral ligament abnormality. *Arthroscopy*. 2016;32(11):2331-2341.
20. Viskontas DG, Giuffre BM, Duggal N, Graham D, Parker D, Coolican M. Bone bruises associated with ACL rupture: correlation with injury mechanism. *Am J Sports Med*. 2008;36(5):927-933.
21. Voskanian N. ACL Injury prevention in female athletes: review of the literature and practical considerations in implementing an ACL prevention program. *Curr Rev Musculoskelet Med*. 2013;6(2):158-163.
22. Yoon KH, Yoo JH, Kim KI. Bone contusion and associated meniscal and medial collateral ligament injury in patients with anterior cruciate ligament rupture. *J Bone Joint Surg Am*. 2011;93(16):1510-1518.
23. Yu B, Garrett WE. Mechanisms of non-contact ACL injuries. *Br J Sports Med*. 2007;41(suppl 1):i47-i51.
24. Zhang L, Hacke JD, Garrett WE, Liu H, Yu B. Bone bruises associated with anterior cruciate ligament injury as indicators of injury mechanism: a systematic review. *Sports Med*. 2019;49(3):453-462.